AIP | Applied Physics Letters

Nanofocusing of longitudinally polarized light using absorbance modulation

Qiang Li, Xing Zhao, Bo Zhang, Yi Zheng, Liqiu Zhou, Lingjie Wang, Yanxiong Wu, and Zhiliang Fang

Citation: Applied Physics Letters **104**, 061103 (2014); doi: 10.1063/1.4864775
View online: http://dx.doi.org/10.1063/1.4864775
View Table of Contents: http://scitation.aip.org/content/aip/journal/apl/104/6?ver=pdfcov
Published by the AIP Publishing

Nanofocusing of longitudinally polarized light using absorbance modulation

Qiang Li,[1] Xing Zhao,[1,a)] Bo Zhang,[1] Yi Zheng,[1] Liqiu Zhou,[1] Lingjie Wang,[2] Yanxiong Wu,[2] and Zhiliang Fang[1]
[1]*Institute of Modern Optics, Key Laboratory of Optical Information Science and Technology, Ministry of Education of China, Nankai University, Tianjin 300071, China*
[2]*Key Laboratory of Optical System Advanced Manufacturing Technology, Changchun Institute of Optics, Fine Mechanics and Physics, Chinese Academy of Sciences, Changchun 130033, China*

(Received 23 November 2013; accepted 28 January 2014; published online 10 February 2014)

Recently, many methods based on amplitude or phase modulation to reduce the focal spot and enhance the longitudinal field component of a tight-focused radially polarized light beam have been suggested. But they all suffer from spot size limit 0.36λ/NA and large side lobes strength in longitudinal component. Here, we report a method of generating a tighter focused spot by focusing radially polarized and azimuthally polarized beams of different wavelengths on a thin photochromic film through a high-numerical-aperture lens simultaneously. In this method, by suppressing the radial component and compressing the longitudinal component of radially polarized beam, absorbance modulation makes the ultimate spot size break the size limit of 0.36λ/NA with side-lobe intensity of longitudinal component below 1% of central-peak intensity. The theoretical analysis and simulation demonstrate that the focal spot size could be smaller than 0.1λ with nearly all radial component blocked at high intensity ratio of the two illuminating beams. [http://dx.doi.org/10.1063/1.4864775]

Over the past decades, radially polarized light beam has attracted growing attentions and lots of theoretical and experimental results have been reported. Owning to the unique characters of strong longitudinal component at the focal plane of a high numerical aperture lens, there are a variety of practical applications with radially polarized beams, especially in near-field such as near-field microscopy,[1–4] near-field second-harmonic generation,[5] plasmon excitation,[6] tip-enhanced Raman spectroscopy,[7] and optical data storage.[8,9]

When a radially polarized beam is focused without any modulation, the electric field components in the focal plane contain the radial component E_r and the longitudinal component E_z.[10] The longitudinal component produces strong intensity along the beam axis, whereas the radial component produces an intensity distribution around the axis, making the spot size bigger than that obtained with linearly or circularly polarized beams.[11,12] However, smaller focal spot with longitudinal component enhancement is highly needed by the applications of radial polarized beams in the field of imaging, sensing, and optical storage. Therefore, many methods using diffraction devices, including amplitude modulation (mainly annular aperture type)[11,13,14] and phase modulation,[15,16] have been implemented to compress the focal spot and enhance the longitudinal component.

By amplitude modulation with annular aperture devices, Quabis *et al*. and Yang *et al*. have achieved a tight-focused spot down to $0.161\lambda^2$ (NA is 0.9) and $0.0711\lambda^2$ (NA is 1.4) in size, respectively.[11,13] Dehez *et al*. also proposed a practical solution to produce a needle of longitudinally polarized light with a transverse width of 0.36λ by choosing a parabolic mirror.[14]

By phase modulation, Wang *et al*. focused a radially polarized Bessel–Gauss beam with a binary optical element and a lens to generate a longitudinally polarized beam needle with a full-width at half-maximum (FWHM) of 0.43λ in the transverse direction.[15] Kalosha and Golub used a combination of a superresolving three-zone plate and a Fresnel diffractive lens to produce a focal spot approaching superresolution allowed subdiffractive limit 0.36λ/NA.[16]

However, the amplitude modulation and the phase modulation all work with diffraction devices. Because electric field in the focal region of a tightly focused radially polarized light is dominated by longitudinal component and its amplitude profile follows a Bessel function of the first kind of order zero $J_0(kr)$, the methods aforementioned are hard to break the size limit of the tightly focused spot of radially polarized light, i.e., 0.36λ/NA, which has been demonstrated by Quabis *et al*., and Grosjean and Courjon.[17,18] Furthermore, the introduction of amplitude or phase modulation diffraction elements have produced intrinsic side lobes in longitudinal component.[11,13–18] The side lobes of longitudinal component degenerate the quality of focused radially polarized beam and lead to a great background noise, which is not preferable to the applications of super-resolution optical data storage, near-field microscopy, lithography, and tip-enhanced Raman spectroscopy.[1,2,7,8,19]

In this letter, we propose a method to generate a tighter focal spot with suppressed side lobes of longitudinal component using absorbance modulation. The proposed method can not only reduce the radial component but also compress the longitudinal component of the radially polarized beam due to near-field effect, which leads to the breaking of the focal spot size limit 0.36λ/NA with the side-lobe intensity of longitudinal component less than 1% of the peak intensity at the center. Calculations show that the FWHM of the focal spot size could be sharply decreased to smaller than $\lambda/10$

a)Author to whom correspondence should be addressed. Electronic mail: zhaoxingtjnk@nankai.edu.cn

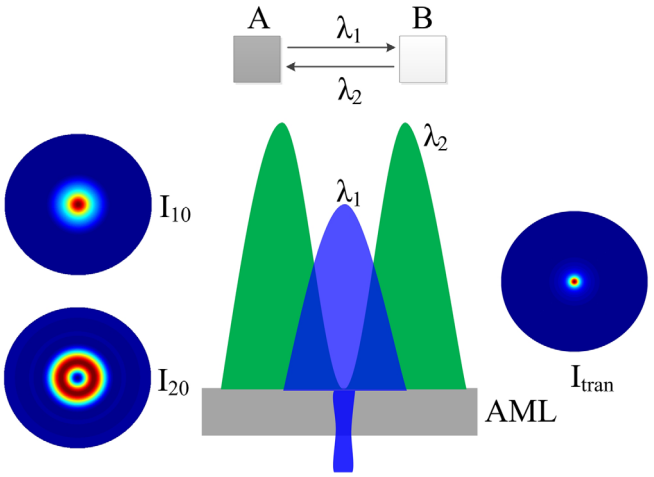

FIG. 1. Scheme of tighter focus for a radially polarized light beam by absorbance modulation. I_{10} and I_{20} are intensity of tightly focused radially polarized light and azimuthally polarized light beam, respectively. I_{tran} is the tighter-focused intensity of radially polarized light after absorbance modulation.

with nearly all radial component blocked at high intensity ratio of the two illuminating beams.

Absorbance modulation was first proposed by Menon and Smith,[20] used for optical lithography, in which a thin film of photochromic material, as absorbance-modulation layer (AML), is placed on top of photoresist and illuminated simultaneously by a focal spot of short wavelength (λ_1) and a ring-shaped illumination of long wavelength (λ_2). The λ_1 radiation converts the photochromic material from configuration A to configuration B, making it transparent to λ_1. The λ_2 radiation converts configuration B back to configuration A, as shown in Fig. 1. Then, a compressed subwavelength transparent aperture for λ_1 is generated in the AML and the photoresist can be exposed by the compressed focal spot of λ_1. It is noted that the compression depends on the intensity ratio of λ_2 to λ_1. Taking azobenzene polymer as photochromic material, one-dimensional grating was achieved experimentally.[21] Using a thermally stable material, results of lines with an average 36 nm width, about one-tenth the illuminating wavelength $\lambda_1 = 325$ nm, were demonstrated in Ref. 22.

It is well known that when a radially polarized light is tightly focused, the total intensity distribution is a central peak with lobes aside, while the intensity distribution of focused azimuthally polarized light is like a doughnut, similar to the radial component of a radially polarized beam.[10,23] If we make tight-focused radially polarized light of short wavelength λ_1 and azimuthally polarized light of long wavelength λ_2 illuminate on AML simultaneously, adopting the thoughts of absorbance modulation, a narrow transmission aperture for λ_1 in the photochromic layer will be produced. Since there is only the longitudinal component in focal spot center, the radial component and side lobes of longitudinal component of the focused radially polarized beam could be greatly suppressed due to the absorbance modulation. Therefore, a tighter focus for a radially polarized light beam with longitudinal component dominant and suppressed side lobes can be realized. The scheme of the method is illustrated in Fig. 1.

According to the vectorial diffraction theory,[10,24] when a radially polarized beam is focused by a high NA lens, The electric field components near the focal plane are formulated as follows:

$$E_r(r,z) = A\int_0^{\alpha} \cos^{1/2}\theta \sin(2\theta) l_0(\theta) J_1(kr\sin\theta) e^{ikz\cos\theta} d\theta, \quad (1)$$

$$E_r(r,z) = 2iA\int_0^{\alpha} \cos^{1/2}\theta \sin^2\theta l_0(\theta) J_0(kr\sin\theta) e^{ikz\cos\theta} d\theta. \quad (2)$$

The electric field components of a focused beam with azimuthally polarized can be expressed as

$$E_\phi(r,z) = 2A\int_0^{\alpha} \cos^{1/2}\theta \sin\theta l_0(\theta) J_1(kr\sin\theta) e^{ikz\cos\theta} d\theta, \quad (3)$$

where α is the angle of the focusing system related to NA, J_0 and J_1 denote the first kind Bessel function of order 0 and 1, respectively. The function $l_0(\theta)$ describes the amplitude distribution, we use uniform illumination in this letter, i.e., $l_0(\theta) = 1$.[25] For all the examples in this paper, NA = 0.9.

When a radially polarized light beam λ_1 and an azimuthally polarized beam λ_2 are simultaneously focused by a high-numerical-aperture lens on AML, these lights can be viewed as photons propagating through the absorptive medium. Following the transport equation proposed by Arridge *et al.*[26,27] and the absorbance model presented in Refs. 17 and 18. Intensity distribution in the photochromic layer can be represented as

$$\frac{\partial I_1(r,z,t)}{\partial z} = -\ln(10)[(\varepsilon_{1A} - \varepsilon_{1B})[A](r,z,t) + \varepsilon_{1B}[A]_0(r,z,t)]I_1(r,z,t), \quad (4)$$

$$\frac{\partial I_2(r,z,t)}{\partial z} = -\ln(10)[(\varepsilon_{2A} - \varepsilon_{2B})[A](r,z,t) + \varepsilon_{2B}[A]_0(r,z,t)]I_2(r,z,t), \quad (5)$$

where ε_A and ε_B are the molar absorption coefficients of A and B configurations. I is the intensity in the layer. The numbers in the subscript represent the wavelength. $[A_0]$ is the initial concentration of A configuration molecule, while $[A]$ is the value in the absorbance-modulation layer. In steady state, $[A]$ is nothing to do with factor t and can be calculated by the formula

$$[A]_{steadystate}(r,z) = \frac{\alpha_{1B}I_1(r,z) + \alpha_{2B}I_2(r,z) + k_{BA}}{(\alpha_{1A} + \alpha_{1B})I_1(r,z) + (\alpha_{2A} + \alpha_{2B})I_2(r,z) + k_{BA}}[A]_0(r,z), \quad (6)$$

where $\alpha_{1A} = \varepsilon_{1A}\phi_{1AB}/E_{M1}, \alpha_{1B} = \varepsilon_{1B}\phi_{1BA}/E_{M1}, \alpha_{2A} = \varepsilon_{2A}\phi_{2AB}/E_{M2}, \alpha_{2B} = \varepsilon_{2B}\phi_{2BA}/E_{M2}$, ϕ is the quantum efficiency, E_{M1} is the energy of 1 mole of photon at λ_1, and k_{BA} is the thermal conversion rate of the AML from state B to state A. The numbers in the subscript represent the wavelength, and the letters AB and BA mean the conversion from the configuration A to B and B to A, respectively.

To prove the feasibility of the proposed method, we use above transport equation and absorbance model to analyze and simulate the characteristics of transmitted light intensity.

In the simulation, the absorbance-modulation layer is composed of azobenzene polymer with the thickness of 200 nm. The material parameters are referred from Refs. 21 and 27. The wavelength of simultaneously focused radially polarized beam and azimuthally polarized beam is $\lambda_1 = 400$ nm and $\lambda_2 = 532$ nm, respectively. Since Menon *et al.* have proved by lithography experiments that the intensity distribution calculated at the bottom surface of the photochromic layer is invariable within certain depth of near field,[21,22] the following simulation and analysis will be implemented at the bottom surface of the photochromic layer as well.

By contrast, the case of radially polarized beam of λ_1 focused alone on the absorbance-modulation layer is analyzed first. Figs. 2(a)–2(c) are the simulation results of the longitudinal component, transverse component and total of the tight-focused radially polarized beam, respectively. Fig. 2(d) is the point spread function (PSF) at the bottom of the photochromic layer.

According to the characteristics of photochromic material, the higher concentration value of A configuration is, the stronger absorbance of λ_1 the material means to be. Consequently, light can transmit from where the concentration value of A configuration is low. Since there is no beam of wavelength λ_2 illuminating on the photochromic layer, the photochromic layer here just acts as a normal absorption layer and absorbance modulation does not happen. Therefore, as Figs. 2(a) and 2(b) shown, both longitudinal and transverse components of tight-focused radially polarized beam can penetrate the photochromic layer, without any compression and suppression. For NA = 0.9, the FWHM of the total electric energy density spot is about 0.74λ (296 nm), and the calculated spot size of longitudinal field alone is 0.49λ (196 nm) with side lobes about 6.4% of the peak intensity.

When the photochromic layer is exposed by tight-focused radially polarized and azimuthally polarized light beams simultaneously, the absorbance modulation occurs. In the nodes center of azimuthally polarized light, only

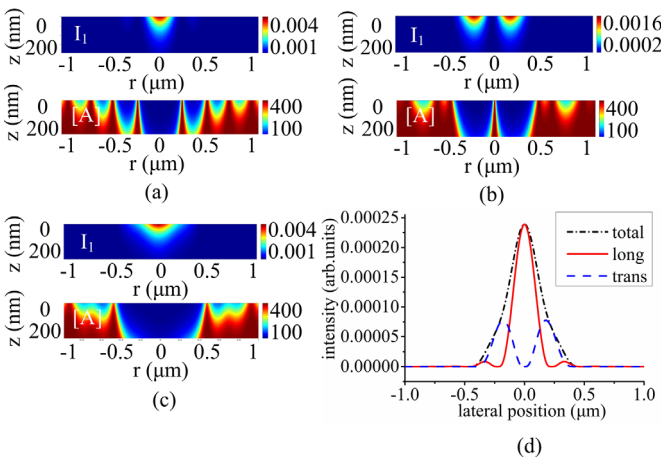

FIG. 2. Absorbance and light intensity distribution in absorbance-modulation layer for (a) longitudinal, (b) transverse, and (c) total components of the radially polarized beam. The top row represents intensity of focused radially polarized beam. The concentration distribution of A configuration molecule of material is shown in the bottom line. (d) PSF at the bottom of the photochromic material layer, when radially polarized light beam exposed alone. Longitudinal, transverse, and total components are shown as solid line, dashed line, and dashed-dotted line, respectively.

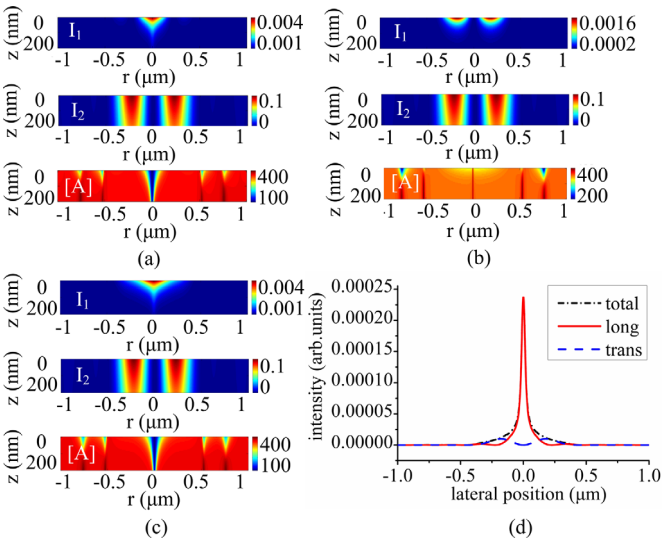

FIG. 3. Absorbance and light intensity distribution in absorbance-modulation layer for (a) longitudinal, (b) transverse, and (c) total components of the radially polarized beam. The top row represents intensity of focused radially polarized beam, central row intensity of focused azimuthally polarized beam, bottom line the concentration distribution of A configuration molecule of material. (d) PSF at the bottom of the photochromic material layer, when radially polarized and azimuthally polarized light beam exposed simultaneously at intensity ratio $I_{02}/I_{01} = 40$. Longitudinal, transverse, and total components are shown as solid line, dashed line, and dashed-dotted line, respectively.

longitudinal component of radially polarized light of λ_1 exits, making the photochromic material convert from configuration A to configuration B and the concentration of configuration A decrease. This leads to the photochromic material in the nodes center transparent to the central longitudinal component of tight-focused radially polarized light. While in the marginal area of the nodes, besides the conversion from configuration A to B excited by λ_1, the increasing intensity of λ_2 makes the photochromic material convert from configuration B back to A simultaneously. The absorbance competition results in the increasing of the concentration of A and the absorption of the longitudinal component, which will be stronger gradually away from the nodes center. Finally, a transmission aperture similar to a funnel appears for longitudinal component, as shown in Fig. 3(a). Owning to the absorbance competing effects between the two beams, a compressed longitudinal component can be achieved at the bottom of the photochromic layer. To be noted here, the compression of the longitudinal component is realized by absorbance modulation, so it will not generate large diffraction side lobes, which is an advantage over conventional methods using diffraction devices.

In the ring-shape area of the focused azimuthally polarized light, the illumination of λ_2 and the transverse field component (radial component) of radially polarized beam in λ_1 makes the photochromic material convert between configuration A and B simultaneously. Due to the higher intensity of λ_2 over λ_1, as shown in Fig. 3(b), the concentration of configuration A in the ring-shape area is much higher, making most of radial component absorbed and blocked. Consequently, the suppressed radial component and compressed longitudinal component result in a highly compressed PSF at the bottom of the photochromic layer, as can be seen in Fig. 3(d).

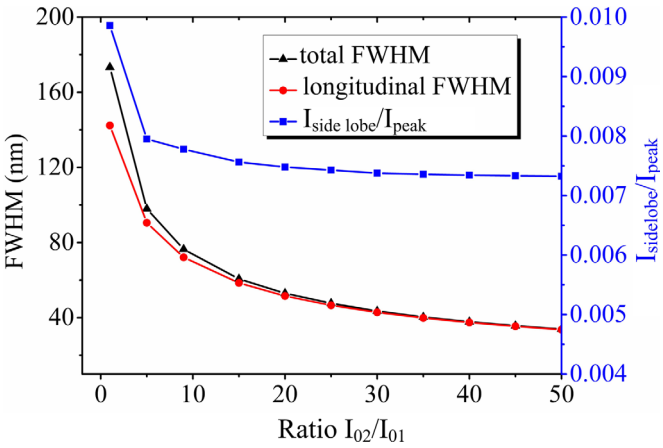

FIG. 4. FWHM as a function of I_{02}/I_{01} for longitudinal component and total components. Red circle represents longitudinal field and black triangle represents total fields. The curve with blue square is the intensity ratio of side lobe to central peak as a function of I_{02}/I_{01} of longitudinal component.

Compared with PSF at the same location shown in Fig. 2(d), both radial component and side lobes of longitudinal component of tight-focused radially polarized beam are suppressed by absorbance modulation with the peak intensity of the longitudinal component remaining. In our simulation, when the intensity ratio I_{02}/I_{01} is 40, the FWHM of total intensity spot is about 0.0945λ (37.8 nm), and the FWHM of the longitudinal field alone is 0.0935λ (37.4 nm) with side lobe less than 0.75% of the peak intensity. The tiny difference between the FWHM of total intensity and longitudinal field means the radial component in the transmitted light is very little.

Since absorbance modulation depends on the intensity ratio of λ_2 to λ_1, the FWHM and intensity ratio of the side lobe to the peak as a function of I_{02}/I_{01} are calculated as well, the results are plotted in Fig. 4. It is shown that the FWHM of longitudinal component and total components decreases with increasing intensity ratio and tends to be consistent. However, there is a difference between them when the ratio is small. This is because of less suppression for radial component during the absorbance competing between the two beams at small ratio, which has been explained in Fig. 3. Even so, the FWHM of longitudinal component is 121 nm as $I_{02}/I_{01} = 3$, which still breaks the focal spot size limit 0.36λ/NA (160 nm). It is indicated from Fig. 4 that the FWHM of longitudinal component could be 40 nm as $I_{02}/I_{01} = 35$, which is one-tenth the illumination wavelength 400 nm. Moreover, the intensity ratio of side lobe to central peak also descends with increasing intensity ratio of λ_2 to λ_1. Nevertheless, the maximal value is below 1%, it is smaller than the value 6.4% before absorbance modulation achieved in Fig. 2(d) and much smaller than that of the conventional methods, which is approximately 20%.[11,13–18]

In conclusion, we proposed a method to generate a tighter focal spot with suppressed side lobes of longitudinal component for a radially polarized light beam using absorbance modulation. In the proposed method, a thin photochromic layer is illuminated by the tight-focused radially polarized light and azimuthally polarized light of different wavelengths simultaneously. Then, a transmitted focal spot with the size breaking the focal spot size limit 0.36λ/NA could be achieved and the intensity of the side lobes of longitudinal component could be below 1% of the peak intensity. By using transport equation and absorbance model, the feasibility of the proposed method is proved. The simulation and analysis results show that the absorbance modulation of the photochromic material could suppress the radial component and compress the longitudinal component of the radially polarized light without large diffraction side lobes generated. The FWHM of the transmitted focal spot size could be sharply decreased to smaller than $\lambda/10$ with nearly all radial component blocked at high intensity ratio of the two illumination beams. Therefore, by contrast with conventional methods using diffraction devices, the proposed method could generate a tighter focal spot with suppressed side lobes of longitudinal component, which will open up extensive application with radially polarized light.

This work was supported by the National Natural Science Foundation of China (NSFC) under Grant No. 61108046, the Research Fund for the Doctoral Program of Higher Education of China under Grant No. 20100031120033, and the Science and Technology Innovation Program of the Chinese Academy of Sciences. X. Zhao wishes to thank C. J. Min, Y. N. Li, and H. T. Liu for their helpful suggestions.

[1]L. Novotny, E. J. Sanchez, and X. S. Xie, Ultramicroscopy **71**, 21 (1998).
[2]A. Bouhelier, M. R. Beversluis, and L. Novotny, Appl. Phys. Lett. **82**, 4596 (2003).
[3]H. Wang, C. J. R. Sheppard, K. Ravi, S. T. Ho, and G. Vienne, Laser Photonics Rev. **6**, 354 (2012).
[4]X. Hao, C. Kuang, Z. Gu, Y. Wang, S. Li, Y. Ku, Y. Li, J. Ge, and X. Liu, Light: Sci. Appl. **2**, e108 (2013).
[5]A. Bouhelier, M. Beversluis, A. Hartschuh, and L. Novotny, Phys. Rev. Lett. **90**, 013903 (2003).
[6]Q. Zhan, Adv. Opt. Photonics **1**, 1 (2009).
[7]N. Hayazawa, Y. Saito, and S. Kawata, Appl. Phys. Lett. **85**, 6239 (2004).
[8]Y. Zhang and J. Bai, Opt. Express **17**, 3698 (2009).
[9]H. Wang, G. Yuan, W. Tan, L. Shi, and T. Chong, Opt. Eng. **46**, 065201 (2007).
[10]K. S. Youngworth and T. G. Brown, Opt. Express **7**, 77 (2000).
[11]R. Dorn, S. Quabis, and G. Leuchs, Phys. Rev. Lett. **91**, 233901 (2003).
[12]G. M. Lerman and U. Levy, Opt. Express **16**, 4567 (2008).
[13]L. X. Yang, X. S. Xie, S. C. Wang, and J. Y. Zhou, Opt. Lett. **38**, 1331 (2013).
[14]H. Dehez, A. April, and M. Piché, Opt. Express **20**, 14891 (2012).
[15]H. Wang, L. Shi, B. Lukyanchuk, C. Sheppard, and C. T. Chong, Nat. Photonics **2**, 501 (2008).
[16]V. P. Kalosha and I. Golub, Opt. Lett. **32**, 3540 (2007).
[17]T. Grosjean and D. Courjon, Opt. Commun. **272**, 314 (2007).
[18]S. Quabis, R. Dorn, M. Eberler, O. Glöckl, and G. Leuchs, Opt. Commun. **179**, 1 (2000).
[19]T. Grosjean and D. Courjon, Opt. Lett. **32**, 976 (2007).
[20]R. Menon and H. I. Smith, J. Opt. Soc. Am. A **23**(9), 2290 (2006).
[21]R. Menon, H.-Y. Tsai, and S. W. Thomas, Phys. Rev. Lett. **98**, 043905 (2007).
[22]T. L. Andrew, H. Y. Tsai, and R. Menon, Science **324**, 917 (2009).
[23]Q. Zhan and J. R. Leger, Opt. Express **10**, 324 (2002).
[24]B. Richards and E. Wolf, Proc. R. Soc. London, Ser. A **253**, 358 (1959).
[25]S. Yew and C. J. R. Sheppard, Opt. Lett. **32**, 3417 (2007).
[26]S. R. Arridge, M. Schweiger, M. Hiraoka, and D. T. Delpy, Med. Phys. **20**, 299 (1993).
[27]H.-Y. Tsai, Ph.D. dissertation (Massachusetts Institute of Technology, 2011).